CHARACTERIZATION OF PHOTODECTORS USING A MONOCHROMATOR AND A BROADBAND LIGHT SOURCE IN THE XYZ COLOR SPACE

J.-S. Botero V.[1,*], F.-E. López G.[1] and J.-F. Vargas B.[2]
[1]Grupo de investigación AEyCC,
Facultad de Ingenierías, Instituto Tecnológico Metropolitano ITM,
Carrera 31 No. 54-10, Medellín, Colombia.
[2]Grupo de Investigación SISTEMIC,
Facultad de Ingeniería, Universidad de Antioquia UdeA
Calle 70 No. 52-21, Medellín, Colombia
E-mail: juanbotero@itm.edu.co, franciscolopez@itm.edu.co, jesus.vargas@udea.edu.co

Submitted: Jan. 5, 2016 ***Accepted: Mar. 31, 2016*** ***Published: June 1, 2016***

Abstract- Photodetectors are sensors, which respond to the electromagnetic radiation of the spectrum. Their spectral response depends on many factors of the manufacturing process, e.g. the type of diode that is used or, in some cases, the optical elements that are added to limit the response band. In this paper, we propose an experimental methodology to obtain the spectral response of a photodetector by constructing the characteristic curve using the monochromatic response. For this purpose, we use a broadband source as input of the monochromator to vary the wavelength each five nm. The characteristic curves of one commercial color sensor were obtained (including the loss) using the output ratio of the monochromator. Via the numerical expression of the response curve, it is possible to model the actual response of the photodetectors to known or simulated spectra of electromagnetic radiation, and thus to generalize photometric measurements. Previously we have demonstrated the importance of obtaining such measurements to study light sources. Finally, this newly developed method helps studying the behavior of a photodetector in detail; hence, it enables the derivation of photometric measurements from known data or simulations.

Index terms*: Photodetector, monochromator, broadband light sources, XYZ color space, RGB sensors.*

I. INTRODUCTION

Photodetectors are sensors that convert electromagnetic energy into an electrical signal. Its function is to show a particular spectral region as output. They are almost always made of semiconductors that are responsive to photo-excitation and include optical filters to limit the response region among other methods of manufacture [1–3]. The visible light is a small segment of the electromagnetic spectrum comprised of wavelengths between 380 nm and 780 nm. Nowadays its research is one of the most important fields worldwide; its influence on our behavior has been widely demonstrated [4–11] and the effect on multiple biological systems such as plants [12–14] and stem cells [15,16], or on food quality [17] is studied. The interest in the study of new applications [18] and the difficulty in taking measurements, which occurs in some cases, have sparked interest in novel models to perform experiments, and to develop light control applications more accurately and at a lower cost. The applications for photodetectors are manifold, the most common are varying photometric measurements [19–21], applications where infrared radiation is utilized [22–26] and where color measurement is required [27–33], intelligent lighting control [19,34–36], the derivation of measures such as CCT (Correlated Color Temperature) [37], the estimation of the CRI (Color Rendering Index) [38] and the determination of power measurements in more particular cases such as PAR (Photosynthetically Active Radiation) [39]. However, the response of low-cost photodetectors is not adjusted to the referred measurements and approximations or transformations are necessary, i.e. calibration models [27,32,33,40] that allow interpreting the output data as a reliable measure. However, this procedure involves extensive experimental work, which is usually done by taking one part of the sample space with known characteristics that allows obtaining the inverse model of the photodetectors. Said inverse model is difficult to generalize, due to the impossibility to determine the full sample space, as in the characterization of light sources [37,38], where it is not possible to include all possible and purchasable light sources while performing the training of the sensor. The same effect occurs when color charts or nonstandard light sources are used for calibrating the color sensors. A further problem is that the adaption of inverse models again requires experimental procedure.

In this paper, a model was developed and implemented to obtain the characteristic curve of low-cost photodetectors using a broadband light source, a monochromator and a high-resolution

spectrometer. Initially the light passes the monochromator and splits into two beams. One of them goes to the spectrometer to measure the power and the other one goes to the photodetector to assess the value of the output signal. This procedure is repeated varying the output wavelength of the monochromator in steps of 10 nm in the visible region absorption spectrum. For each photodetector 41 points are obtained, and then adjusted to compensate the losses occurring in the optical fiber. The monochromator, as well as the source response, are not completely flat; therefore, the beam is split and measured in the spectrometer. The adjusted data represents the spectral response or the characteristic curve of the sensor. The mathematically expressed characteristic curve allows implementing interpolation models of discrete measures from simulated spectra or from known reflectance functions, as in the case of color palettes. The presented methodology reduces the necessity of experiments and allows constructing multiple models from the same photodetector's curve. The datasets of spectra from light sources and reflectance functions of color charts are widely distributed, which allows turning the sensors into measuring devices based on the simulation. As a result of the proposed methodology, the response curve of the TCS3141CS sensor was obtained. The measurement data of the Macbeth color palette was directly obtained with the sensor and the estimated values were obtained with the curve using said methodology (simulated). As a result of the comparison an error below 3.6% error was found. This manuscript is organized as follows: In section 2, the photodetectors, the light source and the spectrometer used for the calibration, are described. Section 3 explains the experimental methodology and the scheme for obtaining the characteristic curve. Section 4 discusses the implemented model and its features. In section 5, the process of interpreting the measurements and the interpolation model is exhibited in detail. And finally, in section 6 conclusions and future prospects of the here presented work are drawn.

II. MATERIALS

a. Broadband source EQ-99

The EQ-99 is a Laser-Driven Light Source (LDLS) UV-VIS-NIR manufactured by ENERGETIQ. This broadband source is specially designed for high brightness and high stability. The spectral output ranges from 170 nm to 2100 nm, with a Numerical Aperture (NA) up to 0.47 and a typical bulb life longer than 5000 h. For the model presented in this article, it is crucial that the light source shows a flat spectral response. Figure 1 shows the spectral response of the LDLS.

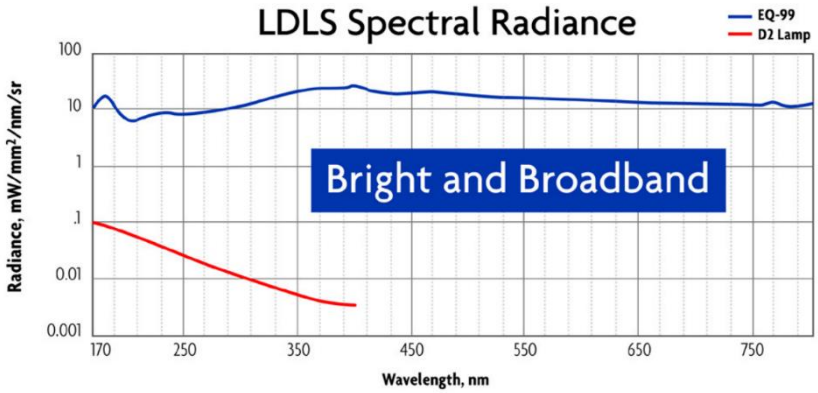

Figure 1. Spectral response LDLS (The image is taken from the manufacturer's datasheet).

b. Monochromator - Mini-Chrom

Mini-Chrom is a monochromator that uses a dial to select the output wavelength. A screw bar mechanism accurately guides the rotation of a diffraction grating, which positions the selected wavelength at the output. The wavelength is read directly in nanometers (nm) by a four-digit counter in all models. The operating range is 200 nm to 800 nm. SMA connectors will be adapted at the input and output for connecting plastic optical fibers.

c. Spectrum Analyzer - AQ6373

The AQ6373 is a Spectrum Analyzer that provides an accurate high-speed analysis of the wavelength range between 350 nm and 1200 nm. This OSA is well suited for general purposes. It also allows USB storage, which saves data in flat format for further analysis.

d. Color sensors - TCS3414CS

TCS3414CS is a color sensor manufactured by Texas Advanced Optoelectronic Solutions (TAOS). It comprises of an 8x2 array of filtered photodiodes, four of them have red filters, four blue, and four green ones; the remaining four are not filtered. Each of the four sensor channels (Red, Green, Blue, and Clear) delivers its output in a format of 16 bits using I2C protocol information at 400 KHz. The gain of the analog converter and the integration time are programmable. The sensor has a synchronization input (SYNC), which allows the precise control of integrated external sources. Table 1 shows some important features of TCS3414CS.

Table 1. Characteristic TCS3414CS

Characteristic	*Value*	*Units*
Sensor	*Photodiode*	$[NA]$
Clock frequency	$0 - 400$	$[KHz]$
A/D Resolution	16	$[bits]$
Operating voltage	$2.7 - 3.6$	$[V]$
Supply Current ($V_{DD} = 3.6$)	*8.7-11*	$[mA]$
Operating temperature	$-40 - 85$	$[°C]$
Communication	*I2C*	$[NA]$
Chanels	*R, G, B, clear*	$[NA]$

e. Experiment

In Figure 2 the explanatory diagram of the proposed experiment is presented. Below its parts are described:

1. The system input is a white light source EQ-99 (polychromatic) with UV-VIS-NIR emission.
2. The white light enters a mechanical UV-VIS-NIR monochromator (Mini-Chrom) that selects the desired wavelength. Adjusting said wavelength is carried out manually with a mechanical element at intervals of 10 nm in the visible spectrum (380-780 nm).
3. The output of the monochromator must be demultiplexed into two identical outputs. One of them is led to the spectrometer, as a reference value, and the second one to the photodetector to be evaluated.
4. The values obtained in the previous phase will allow to know, first, the gain of the photodetector at a certain wavelength and, second, the total VIS-NIR scan (point to point) to reconstruct the spectral response curve of the photodetector.

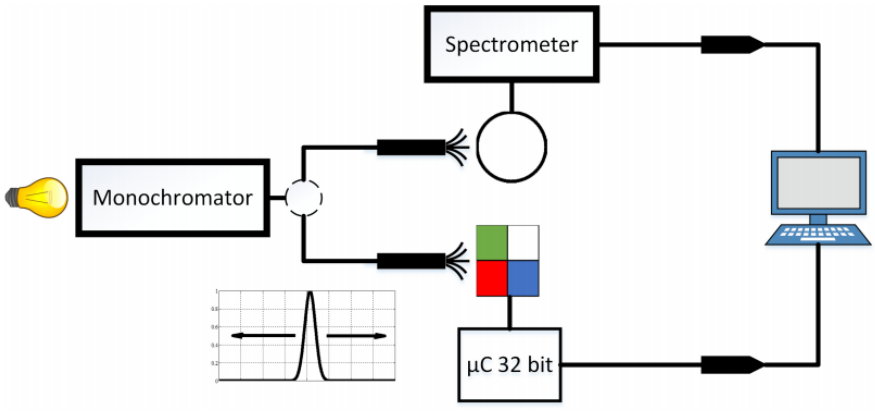

Figure 2. Experiment of calibration

f. CIE standard observer matching functions

Values in the color space X, Y, Z of a surface can be obtained using the model shown in equation 1. Where $E(\lambda)$ represents the source, $P(\lambda)$ the reflectance curve and $x(\lambda)$, $y(\lambda)$ and $z(\lambda)$ the curve of the observer.

$$X = k \sum_{\lambda=380}^{780} E(\lambda) \cdot \tilde{x}(\lambda) \cdot P(\lambda) d\lambda$$

$$Y = k \sum_{\lambda=380}^{780} E(\lambda) \cdot \tilde{y}(\lambda) \cdot P(\lambda) d\lambda \quad (1)$$

$$Z = k \sum_{\lambda=380}^{780} E(\lambda) \cdot \tilde{z}(\lambda) \cdot P(\lambda) d\lambda$$

g. Color checker

The color checker is a color palette with 24 samples arranged in 4 rows. The reflectance of the samples are known, allowing to use it as a reference standard. In the **Figure 3** the distribution of the colors is shown. With the reflectance information of the Color Checker and given that the source spectrum is known, one can calculate the value of the XYZ space using Equation 1.

Figure 3. Macbeth Chart

III. SOLUTION

a. Spectral response of the sensor

In principle and using the model described in **Figure 2** in particular, the spectra are obtained at the exit of the monochromator. Measurements of spectra were taken every 10 nm in the range between 380 nm and 780 nm to a total value of 41 spectra and repeated four times. As shown in **Figure 4** the spectra are narrow allowing for improved estimation of the response model to be generated. The peak values obtained in this step enable the estimation of the normalized response of the sensor (each channel) to each of the 41 points. With the normalized monochromator output values, the TCS3414CS sensor response was evaluated.

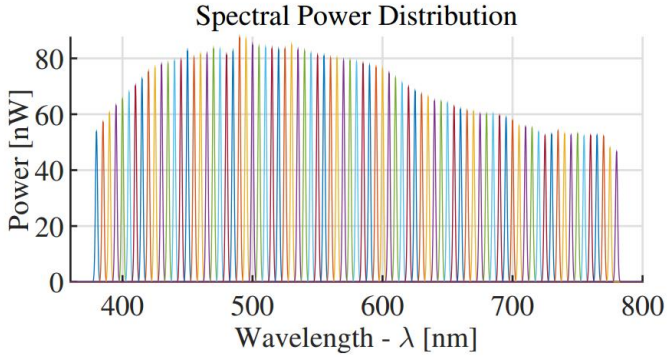

Figure 4. Output monochromator - experimental result

As mentioned, the values shown in Figure 4 (peaks) are needed to obtain the gain of each of the photodetectors for each one of the RGB channels. The spectral response curve obtained at the end of the process is presented in Figure 5. It corresponds to the one provided by the manufacturer. In total, there are 41 reference points per channel that can be used to perform simulations of the sensor response when they are stimulated with known spectra.

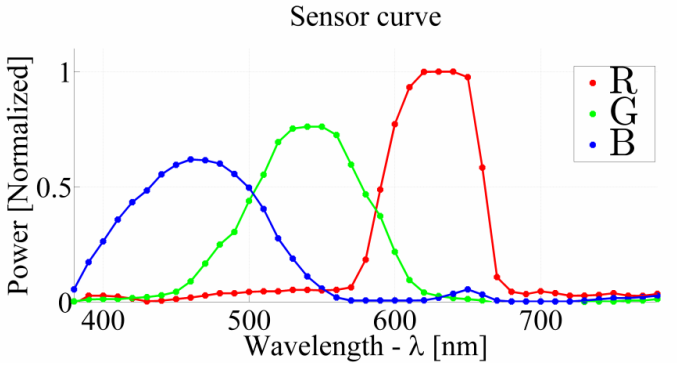

Figure 5. Sensor Response - experimental result

To evaluate the data in the theoretical model, it is necessary to know the spectrum of the light source that will accompany the color sensor for measurement (**Figure 6**), i.e. $E(\lambda)$ in (1).

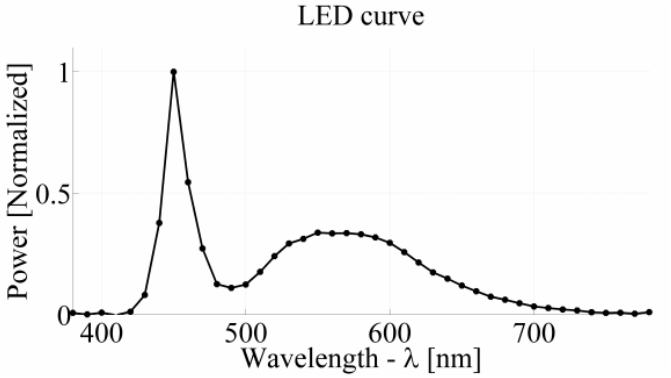

Figure 6. LED curve - experimental result

Table 2 shows the values from the XYZ measurements using the sensor on the color checker (XM, YM, ZM) and using the response curve found with the proposed methodology (XE, YE, ZE).

Table 2. XYZ space Color Checker

Color	XE	XM	YE	YM	ZE	ZM
01 Dark Skin	0,136	0,134	0,119	0,120	0,082	0,081
02 Light Skin	0,430	0,427	0,350	0,330	0,258	0,255
03 Blue Sky	0,138	0,134	0,231	0,230	0,302	0,290
04 Foliage	0,111	0,098	0,173	0,160	0,093	0,081
05 Blue Flower	0,220	0,219	0,274	0,280	0,385	0,382
06 Bluish Green	0,219	0,219	0,509	0,491	0,424	0,429
07 Orange	0,467	0,475	0,290	0,280	0,100	0,093
08 Purplish Blue	0,098	0,098	0,164	0,160	0,344	0,336
09 Moderate Red	0,377	0,390	0,164	0,170	0,141	0,151
10 Purple	0,096	0,098	0,082	0,090	0,127	0,127
11 Yellow Green	0,305	0,329	0,495	0,501	0,164	0,185
12 Orange Yellow	0,505	0,524	0,424	0,420	0,119	0,127
13 Blue	0,051	0,049	0,094	0,098	0,246	0,243
14 Green	0,121	0,122	0,285	0,280	0,128	0,127
15 Red	0,300	0,293	0,098	0,100	0,072	0,070
16 Yellow	0,603	0,622	0,628	0,611	0,163	0,174
17 Magenta	0,372	0,378	0,177	0,200	0,269	0,278
18 Cyan	0,097	0,098	0,260	0,260	0,364	0,359
19 White	0,756	0,792	1,000	0,981	0,878	0,881
20 Neutral 8	0,490	0,512	0,654	0,661	0,581	0,603
21 Neutral 6.5	0,308	0,317	0,415	0,410	0,368	0,382
22 Neutral 5	0,175	0,171	0,233	0,220	0,204	0,197
23 Neutral 3.5	0,089	0,085	0,121	0,120	0,108	0,104
24 Black	0,039	0,037	0,052	0,050	0,047	0,046

Finally, in Table 3, the estimation error for each channel, and each sample is presented. The highest error value is 0.0036 (the error is normalized) and occurs in white color, the error is low, considering that was used a low cost sensor. The measurement error is expected due to the resolution of the spectral response curve (10 nm), however the experiment demonstrates the effectiveness of the curve to use simulated data and to interpolate measures with the sensor.

Table 3. XYZ space Color Checker - error

Color	ER-X	ER-Y	ER-Z
01 Dark Skin	0,000	0,001	0,001
02 Light Skin	0,003	0,020	0,003
03 Blue Sky	0,004	0,001	0,012
04 Foliage	0,013	0,013	0,012
05 Blue Flower	0,000	0,006	0,002
06 Bluish Green	0,000	0,019	0,004
07 Orange	0,008	0,010	0,007
08 Purplish Blue	0,001	0,003	0,007
09 Moderate Red	0,014	0,006	0,009
10 Purple	0,002	0,009	0,000
11 Yellow Green	0,024	0,005	0,021
12 Orange Yellow	0,020	0,003	0,009
13 Blue	0,002	0,004	0,003
14 Green	0,001	0,005	0,001
15 Red	0,008	0,003	0,003
16 Yellow	0,019	0,018	0,011
17 Magenta	0,006	0,023	0,009
18 Cyan	0,001	0,001	0,005
19 White	0,036	0,019	0,002
20 Neutral 8	0,022	0,006	0,022
21 Neutral 6.5	0,009	0,005	0,014
22 Neutral 5	0,004	0,012	0,007
23 Neutral 3.5	0,004	0,000	0,004
24 Black	0,002	0,002	0,001
	0,009	**0,008**	**0,007**

IV. CONCLUSIONS

This paper presents a methodology for determining the spectral response of photodetectors. Its efficacy was demonstrated by measuring the color directly on a standardized color palette and comparing this data with the values obtained from the simulation using the photodetector response curve found with the proposed methodology, with the reflectance curves, and with the SPD of the light source.

The applications arising from knowing the characteristic curve of low-cost photodetectors extend to all problems where it is necessary to find transformation models for output values and the simulated stimulation data is known, for example, deriving models for measurements of CCT or CRI with a color sensor using simulated spectra.

V. Acknowledgments

This work is part of the research project "Developing a methodology for obtaining experimental spectral response of low cost photodetectors to derive photometric measurements" with ID P14207, of the Automática, Electrónica y Ciencias Computacionales Group COL0053581. Instituto Tecnológico Metropolitano, Medellín-Colombia. The authors thank CODI, "Estrategia de sostenibilidad from Universidad de Antioquia" for the support to develop this work.

REFERENCES

[1] M. a Martínez, E.M. Valero, J. Hernández-Andrés, J. Romero, G. Langfelder, Combining transverse field detectors and color filter arrays to improve multispectral imaging systems., Appl. Opt. 53 (2014) C14–C24. doi:10.1364/AO.53.000C14.

[2] G. Langfelder, Spectrally reconfigurable pixels for dual-color-mode imaging sensors, Appl. Opt. 51 (2012) A91–A98. doi:10.1364/AO.51.000A91.

[3] H. Escid, M. Attari, M. Ait, W. Mechti, 0 . 35 µm CMOS optical sensor for an integrated transimpedance circuit, Int. J. Smart Sens. Intell. Syst. 4 (2011) 467–481.

[4] ASSIST, Recommendations for Specifying Color Properties of Light Sources for Retail Merchandising, Lighthing Research Center, 2010.

[5] K.. Biron, C.M.H. Demers, Perceptual Interactions between Light and Architecture: A graphical vocabulary using models and photographs, in: PLEA2009, Quebec, 2009.

[6] Á. Logadóttir, S. a. Fotios, J. Christoffersen, S.S. Hansen, D.D. Corell, C. Dam-Hansen, Investigating the use of an adjustment task to set preferred colour of ambient illumination, Color Res. Appl. 38 (2013) 46–57. doi:10.1002/col.20714.

[7] F. Behar-Cohen, C. Martinsons, F. Viénot, G. Zissis, A. Barlier-Salsi, J.P. Cesarini, et al., Light-emitting diodes (LED) for domestic lighting: Any risks for the eye?, Prog. Retin. Eye Res. 30 (2011) 239–257. doi:10.1016/j.preteyeres.2011.04.002.

[8] H. Li, X. Mao, Y. Han, Y. Luo, Wavelength dependence of colorimetric properties of lighting sources based on multi- color LEDs, Opt. Express. 21 (2013) 3775–3783. doi:10.1364/OE.21.003775.

[9] F.S. Yılmaz, C. Ticleanu, G. Howlett, S. King, P.J. Littlefair, People-friendly lighting controls – User performance and feedback on different interfaces, Light. Res. Technol. (2015) 1477153515583180. doi:10.1177/1477153515583180.

[10] J. Schhanda, P. Csuti, F. Szabo, P. Bhusal, L. Halonen, Introduction to a study of preferred colour rendering of light sources, Light. Res. Technol. 47 (2015) 28–35. doi:10.1177/1477153513514426.

[11] T.P. State, T. Hong, K. Polytechnic, H. Kong, P. Corporation, K. City, et al., Colour preference varies with lighting application, Light. Res. Technol. (2015) 1–13.

[12] I. Gómez, E. Pérez-Rodríguez, B. Viñegla, F.L. Figueroa, U. Karsten, Effects of solar radiation on photosynthesis, UV-absorbing compounds and enzyme activities of the green alga Dasycladus vermicularis from southern Spain, J. Photochem. Photobiol. B Biol. 47 (1998) 46–57. doi:10.1016/S1011-1344(98)00199-7.

[13] P. Pinho, T. Rosvall, E. Tetri, L. Halonen, Light emitting diodes in plant growth: comparative growth test in greenhouse and evaluation of photosynthetic radiation, (2008).

[14] J. Torres-Sánchez, F. López-Granados, J.M. Peña, An automatic object-based method for optimal thresholding in UAV images: Application for vegetation detection in herbaceous crops, Comput. Electron. Agric. 114 (2015) 43–52. doi:10.1016/j.compag.2015.03.019.

[15] W.-K. Ong, H.-F. Chen, C.-T. Tsai, Y.-J. Fu, Y.-S. Wong, D.-J. Yen, et al., The activation of directional stem cell motility by green light-emitting diode irradiation., Biomaterials. 34 (2013) 1911–20. doi:10.1016/j.biomaterials.2012.11.065.

[16] S. Yoshida, T. Mandel, C. Kuhlemeier, Stem cell activation by light guides plant organogenesis, Genes Dev. 25 (2011) 1439–50. doi:10.1101/gad.631211.

[17] D. Wu, D.-W. Sun, Colour measurements by computer vision for food quality control – A review, Trends Food Sci. Technol. 29 (2013) 5–20. doi:10.1016/j.tifs.2012.08.004.

[18] D. Bhattacharjee, G. Sharma, R. Bera, Universal intelligent sensor interface, Int. J. Smart Sens. Intell. Syst. 8 (2015) 2307–2327.

[19] S. Matta, S.M. Mahmud, An intelligent light control system for power saving, in: IECON 2010-36th Annu. Conf. IEEE Ind. Electron. Soc., IEEE, 2010: pp. 3316–3321.

[20] M. Miki, Y. Kasahara, T. Hiroyasu, M. Yoshimi, Construction of Illuminance Distribution Measurement System and Evaluation of Illuminance Convergence in Intelligent Lighting System, in: IEEE SENSORS 2010 Conf., IEEE, 2010: pp. 2431–2434.

[21] Y.-J. Wen, J. Granderson, A.M. Agogino, Towards Embedded Wireless-Networked Intelligent Daylighting Systems for Commercial Buildings, IEEE Int. Conf. Sens. Networks, Ubiquitous, Trust. Comput. (2006) 326–331. doi:10.1109/SUTC.2006.1636196.

[22] M. Attas, E. Cloutis, C. Collins, D. Goltz, C. Majzels, J.R. Mansfield, et al., Near-infrared spectroscopic imaging in art conservation: investigation of drawing constituents, J. Cult. Herit. 4 (2003) 127–136. doi:10.1016/S1296-2074(03)00024-4.

[23] E.M. Gorostiza, J.L.L. Galilea, F.J.M. Meca, D.S. Monzú, F.E. Zapata, L.P. Puerto, Infrared sensor system for mobile-robot positioning in intelligent spaces., Sensors. 11 (2011) 5416–38. doi:10.3390/s110505416.

[24] Y. Le Maoult, T. Sentenac, J.J. Orteu, J.P. Arcens, Fire Detection, Process Saf. Environ. Prot. 85 (2007) 193–206. doi:10.1205/psep06035.

[25] C.-C. Tong, K.-L. Wen, Y.-T. Wang, S.-J. Lin, The development of portable infrared color sensor, in: Ind. Technol. 2005. ICIT 2005. IEEE Int. Conf., IEEE, 2005: pp. 959–962.

[26] T. Fu, H. Zhao, J. Zeng, Z. Wang, M. Zhong, C. Shi, Improvements to the three-color optical CCD-based pyrometer system, Appl. Opt. 49 (2010) 5997–6005. doi:10.1364/AO.49.005997.

[27] J.E. Agudo, P.J. Pardo, H. Sánchez, A.L. Pérez, M.I. Suero, A low-cost real color picker based on arduino., Sensors (Basel). 14 (2014) 11943–56. doi:10.3390/s140711943.

[28] G.C. Anzalone, A.G. Glover, J.M. Pearce, Open-source colorimeter., Sensors (Basel). 13 (2013) 5338–46. doi:10.3390/s130405338.

[29] J.S. Bajić, D.Z. Stupar, B.M. Dakić, M.B. Živanov, L.F. Nagy, An absolute rotary position sensor based on cylindrical coordinate color space transformation, Sensors Actuators A Phys. 213 (2014) 27–34. doi:10.1016/j.sna.2014.03.036.

[30] K.-C. Lee, S.-H. Moon, B. Berkeley, S.-S. Kim, Optical feedback system with integrated color sensor on LCD, Sensors Actuators A Phys. 130-131 (2006) 214–219. doi:10.1016/j.sna.2006.01.028.

[31] M. Moghavvemi, S.S. Jamuar, E.H. Gan, Y.C. Yap, Design of low cost flexible RGB color sensor, in: IEEE (Ed.), 2012 Int. Conf. Informatics, Electron. Vis., IEEE, Dhaka, 2012: pp. 1158–1162. doi:10.1109/ICIEV.2012.6317416.

[32] Ö.G. Saracoglu, H. Altural, Color Regeneration from Reflective Color Sensor Using an

Artificial Intelligent Technique, Sensors (Basel). 10 (2010) 8363–8374. doi:10.3390/s100908363.

[33] A. Sen, J. Albarella, J. Carey, P. Kim, W. McNamara III, Low-cost colorimetric sensor for the quantitative detection of gaseous hydrogen sulfide, Sensors Actuators B Chem. 134 (2008) 234–237. doi:10.1016/j.snb.2008.04.046.

[34] M. Aldrich, N. Zhao, J.A. Paradiso, Energy efficient control of polychromatic solid state lighting using a sensor network, in: SPIE 7784, Tenth Int. Conf. Solid State Light., SPIE, 2010. doi:10.1117/12.860755.

[35] M. Ashibe, M. Miki, T. Hiroyasu, Distributed optimization algorithm for lighting color control using chroma sensors, in: 2008 IEEE Int. Conf. Syst. Man Cybern., IEEE, Singapore, 2008: pp. 174–178. doi:10.1109/ICSMC.2008.4811270.

[36] J.-S. Botero V., F.-E. Lopez G., J.-F. Vargas B., Classification of artificial light sources and estimation of Color Rendering Index using RGB sensors , K Nearest Neighbor and Radial Basis Function, Int. J. Smart Sens. Intell. Syst. 8 (2015) 1505–1524.

[37] J.-S. Botero V., F.-E. Lopez G., J.-F. Vargas B., Calibration method for Correlated Color Temperature (CCT) measurement using RGB color sensors, in: Image, Signal Process. Artif. Vis. (STSIVA), 2013 XVIII Symp., IEEE, Bogotá, 2013: pp. 3–8. doi:10.1109/STSIVA.2013.6644921.

[38] J.-S. Botero V., F.-E. Lopez G., J.-F. Vargas B., Calibration Method for Measuring the Color Rendering Index (CRI) using RGB Sensor, Tecnológicas. EE (2013) 325–338.

[39] J.-S. Botero V., S.-M. Navarro, N. Giraldo, L. Atehortua, Estimation of Photosynthetically Active Radiation (PAR) using a low cost spectrometer, IEEE Lat. Am. Trans. 12 (2014) 107–111. doi:10.1109/TLA.2014.6749525.

[40] M. Assaad, I. Yohannes, A. Bermak, D. Ginhac, F. Meriaudeau, Design and characterization of automated color sensor system, Int. J. Smart Sens. Intell. Syst. 7 (2014) 1–12.